Konversi Energi dan Manufaktur

P-ISSN : 2339-2029
E-ISSN : 2622-5565

Jurnal Konversi Energi dan Manufaktur
Volume 11 Number 2 – July 2026 Page 170-181
Website : http://journal.unj.ac.id/unj/index.php/jkem
DOI: https://doi.org/10.21009/JKEM.11.2.7

Computational Fluid Dynamics Analysis of the Effect of Stern Shape Modifications on Ship Resistance

Julyus Acang Suwignyo Putro[1], I Putu Sindhu Asmara[1], Priyambodo Nur Ardi Nugroho[1*]
[1] *Ship Design and Construction Engineering, Politeknik Perkapalan Negeri Surabaya, Jawa Timur, 60111, Indonesia.*
* Corresponding Author. E-mail : priyambodo@ppns.ac.id

Article information - : Received : 10-06-2026; Revised : 14-07-2026; Accepted : 18-07-2026

Abstract

The change of the propulsion system usually involves structural modifications of the stern, which have a large impact on the hydrodynamic behaviour of the ship, e.g. the total resistance and the flow field. Calculations of the drag force and flow velocity are performed in order to investigate the effect of the stern modifications on the vessel resistance. The study was carried out by means of Computational Fluid Dynamics (CFD) simulations in the ANSYS Workbench environment. The research compared four different skeg size variants used after modification of the original hull of the ship. The simulation results show that the flow velocity of the original hull was 3.220 m/s and the drag force was 118.70 kN. Among the tested variations, variation 4 emerged as the most efficient design, yielding a reduced drag force of 81.59 kN and an increased flow velocity of 3.461 m/s. Ultimately, the proposed stern modification successfully lowered the total ship resistance from 118.70 kN to 82.93 kN, achieving a significant 30% reduction in resistance.

Keywords: hull optimization; resistance reduction; self-propelled oil barge; wake flow.

1. Introduction

Ship resistance is a fundamental parameter in naval architecture, directly impacting fuel consumption, engine load, and overall operational efficiency [1]. In the maritime industry, the demand for vessel modifications is increasing, particularly when existing ships undergo repowering or propulsion system upgrades to meet modern performance standards [2]. Such modifications frequently need structural changes to the stern geometry to accommodate new equipment or improve flow characteristics [3]. Since the stern region dictates the wake field and water flow toward the propeller, any geometric alteration can significantly influence the vessel's hydrodynamic performance [4]. Therefore, understanding the relationship between stern shape modifications and total resistance is crucial for ensuring the economic and technical viability of ship conversion projects.

The self-propelled oil barge (SPOB) is a specialized type of oil tanker equipped with its own propulsion system, designed to distribute fuel to areas with limited water depth or small coastal depots [5]. In Indonesia, the SPOB fleet plays a strategic role in ensuring the smooth operation of the national energy supply chain across the archipelago [6]. To improve operational efficiency, many SPOB units, like in Figure 1 undergo significant modifications, particularly to the stern, to accommodate new propulsion systems or internal engine room adjustments following previous accident [7]. However, structural modifications in the stern area are critical; imprecise geometric changes can disrupt fluid flow toward the propeller and significantly increase the ship's total resistance [8]. Consequently, analyzing the impact of stern shape changes on SPOB vessels is vital to ensure that modifications maintain optimal hydrodynamic performance.

P-ISSN : 2339-2029
E-ISSN : 2622-5565

Jurnal Konversi Energi dan Manufaktur
Volume 11 Number 2 – July 2026 Page 170-181
Website : http://journal.unj.ac.id/unj/index.php/jkem
DOI: https://doi.org/10.21009/JKEM.11.2.7

Figure 1. SPOB Ratu Yamani

Computational fluid dynamics (CFD) has become an essential tool in evaluating ship performance, offering high accuracy comparable to traditional experimental towing tank testing at a lower cost [9]. Previous research has explored various hull optimization techniques [10], [11], such as the implementation of bulbous bows to reduce wave-making resistance [12] or the adjustment of hull lines to minimize pressure drag [13]. Additionally, the use of skegs has been extensively documented in maritime literature, primarily focusing on their role in enhancing the course stability of barges and specialized vessels [14], [15]. Studies on stern flow have further emphasized the role of pressure distribution and flow separation in determining the viscous resistance components of a ship [16].

Modern advancements in maritime engineering prioritize the optimization of existing vessel hulls to extend their service life and reduce environmental footprints. While many studies focus on optimizing the hull form of large container ships or tankers from the design stage [17], the specific impact of incremental skeg size variations on the resistance of smaller vessels—particularly those undergoing localized stern reconstruction—is less frequently addressed in detail. Current state-of-the-art CFD simulations, specifically using environments like ANSYS Workbench, allow for precise sensitivity analysis of these geometric changes [18]. This allows researchers to model the complex interaction between the modified hull and the fluid flow with a high degree of fidelity, identifying optimal configurations that were previously difficult to verify without physical prototypes.

Most current literature focuses on either entirely new hull designs [19] or standard appendages for directional stability [20]. While some researchers have investigated general stern flow, there have been limited studies that examine field-based stern retrofits of SPOB vessels using comparative CFD analysis of skeg geometry variations. Specifically, previous research often emphasizes skeg volume, whereas the novelty of this study lies in analyzing how subtle changes to the skeg shape and geometry, while maintaining relatively similar volumes, impact drag force and stern flow characteristics. Therefore, this research focuses on the modification of a ship's stern by analyzing four different skeg geometry variations to minimize total resistance. This research intends to evaluate the drag force and flow velocity through numerical simulations. The objectives of this research are to compare the hydrodynamic performance of the original hull with the modified variations and to identify the most efficient stern configuration that provides a significant reduction in resistance

2. Experimental Methods

2.1. CFD Setup

The numerical simulations were conducted using the ANSYS Workbench environment, specifically utilizing the FLUENT solver. The analysis process was structured into five primary stages: Geometry, Meshing, Setup, Solution, and Result.

Konversi Energi dan Manufaktur
P-ISSN : 2339-2029
E-ISSN : 2622-5565
Jurnal Konversi Energi dan Manufaktur
Volume 11 Number 2 – July 2026 Page 170-181
Website : http://journal.unj.ac.id/unj/index.php/jkem DOI: https://doi.org/10.21009/JKEM.11.2.7

The computational domain was defined to surround the hull, with inlet and outlet boundaries set at a distance to allow for proper flow development as seen in Figure 2. The hull model was processed in Rhinoceros 6.0 to ensure a solid model structure, preventing fluid from entering the hull during analysis.

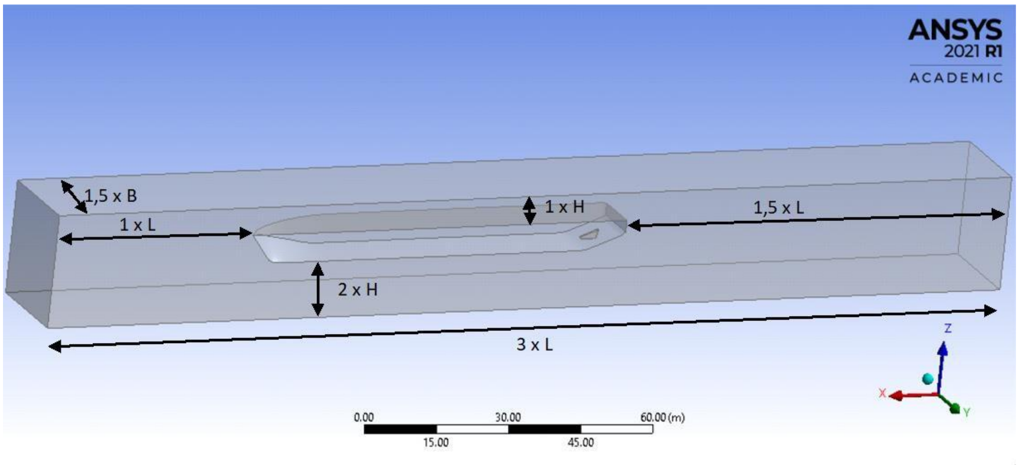

Figure 2. Domain geometry

The domain was discretized using an unstructured mesh approach, with refinements applied to the stern and skeg regions where flow gradients are highest. The mesh result could be seen in Figure 3. The simulations utilized the Standard k−ϵ turbulence model to account for viscous effects and flow behavior, as this model is widely adopted in marine CFD applications for its robustness in predicting mean flow characteristics and turbulence intensities around complex hull geometries.

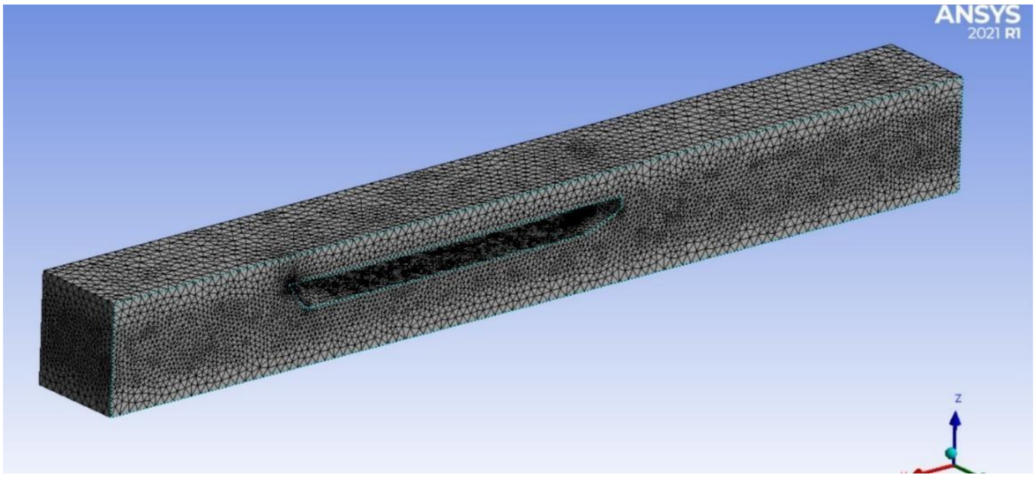

Figure 3. Meshing process result

The boundary conditions were defined by setting the inlet as a pressure inlet with a specified velocity corresponding to the ship's service speed of 8 knots (4.115 m/s) and a water depth of 16.942 m. Meanwhile, the outlet was configured to allow for flow exit, maintaining consistency with the inlet parameters. Additionally, the hull was treated as a no-slip wall boundary. The solver was configured for steady-state analysis, with convergence criteria monitored by tracking the residuals of momentum, continuity, and turbulence equations, and iterations continued until the solution reached a stable, converged state.

To ensure that the numerical results are independent of the mesh resolution and to quantify numerical uncertainty, a grid convergence study was conducted. Three different mesh densities—coarse, medium, and fine—were generated for the baseline hull model. The drag force (R_T) was computed for each mesh resolution to determine the Grid Convergence Index (GCI). As shown in Table 1, the variation in drag force between the medium and fine mesh was less than 1%, indicating that the medium mesh density provides sufficient accuracy while maintaining computational efficiency.

Table 1. Mesh density

Mesh type	Number of elements	Drag force (kN)	Relative difference (%)
Coarse	1200000	121.52	-
Medium	2400000	118.70	2.32
Fine	4800000	118.45	0.21

Based on these results, the medium mesh density (2.4 million elements) was selected for all subsequent simulations of the stern variations. This convergence analysis confirms that the numerical uncertainty is within acceptable limits for engineering predictions, ensuring that the observed 31.2% resistance reduction is attributable to geometric modifications rather than discretization errors.

2.2. Ship Dimension

This research employs a numerical approach using CFD to analyze ship resistance. The primary object of this study is a SPOB before and after stern modification. The original vessel (LOA 87.113 m, C_b 0.85) was modified by extending the stern length by 2.6 m and adding a skeg and engine bed to accommodate a new propulsion system, resulting in a modified hull (LOA 89.713 m, C_b 0.86). The detailed principal dimensions of the ship before and after these modifications are presented in Table 2. To determine the optimal hydrodynamic performance, four skeg size variations were developed based on field data, with dimensions varying in height, length, and width as detailed in the technical specifications of the modification project.

2.3. Hull Modelling

The hull modelling was performed by transforming the principal dimension data listed in Table 2 into a three-dimensional geometry as seen in Figure 4. This process began by inputting key parameters such as Length Between Perpendiculars (LBP), Breadth (B), Draft (T), and Block Coefficient (C_b) into the Maxsurf Modeller software. The determination of the hull curves (lines plan) focused on the stern area to ensure that volume changes resulting from the 2.6-meter extension and skeg modifications were hydrostatically accurate. The precision of this modeling is critical, as any geometric deviation from the actual principal dimensions would directly affect the pressure distribution and fluid flow patterns in the subsequent CFD simulation stages.

Table 2. Principal dimensions of the vessel before and after modification

No.	Dimensions	Before	After
1	Length overall (LOA)	87.113 m	89.713 m
2	Length waterlines (LWL)	84.180 m	86.840 m
3	Breadth (B)	21.946 m	21.946 m
4	Depth (H)	6.096 m	6.096 m
5	Draft (T)	4.750 m	4.750 m
6	Speed (Vs)	8 knots	8 knots
7	C_b	0.85	0.86

The numerical modeling process followed a multi-stage software workflow. The initial hull forms were designed using Maxsurf Modeller Advance to ensure hydrostatic accuracy. These surface models were then exported to Rhinoceros 6.0 to be converted into solid geometries, preventing fluid penetration into the hull during simulation. The final solid models were imported into the ANSYS Workbench environment for CFD analysis. The simulation domain was constructed as a computational towing tank (domain) around the hull, with dimensions determined by the vessel's speed and length to minimize boundary interference.

Konversi Energi dan Manufaktur
P-ISSN : 2339-2029
E-ISSN : 2622-5565
Jurnal Konversi Energi dan Manufaktur
Volume 11 Number 2 – July 2026 Page 170-181
Website : http://journal.unj.ac.id/unj/index.php/jkem
DOI: https://doi.org/10.21009/JKEM.11.2.7

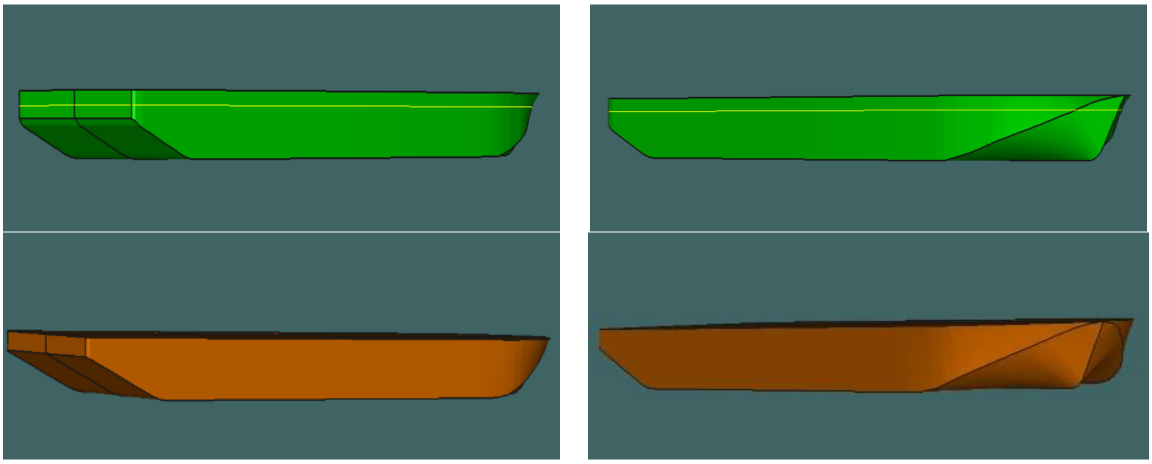

Figure 4. Hull modeling before (top) and after modification (bottom) using Maxsurf Modeller

2.4. Skeg Variation

This stage focuses on integrating skeg components into the previously developed base hull models. For the pre-modification hull, skeg components were positioned at the stern on both the port and starboard sides, with dimensions derived from actual field data. Meanwhile, for the post-modification model, the modeling included both the skegs and the engine bed structure.

In this study, four variations of skeg dimensions were established to evaluate their influence on vessel performance. Variation 1 adopted the actual dimensions from field data post-modification, which then served as the reference parameter for determining the dimensions of the other three skeg variations. The visual placement of these components for both conditions is illustrated in Figure 5. Detailed dimensional specifications for the field data and the four skeg variations are comprehensively presented in Table 3.

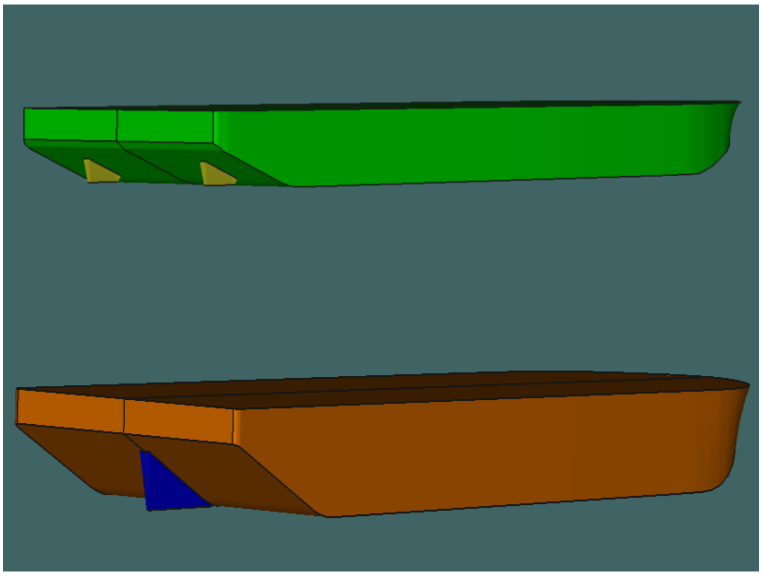

Figure 5. Skeg modeling before modification (top) and after modification (bottom)

The skeg modeling stage aims to integrate supporting components into the previously developed base hull models. For the pre-modification hull model, the addition was limited to the skeg components located on the port and starboard sides of the vessel's stern, using dimensions derived from actual field data. In contrast, modeling for the post-modification vessel involved adding both the skegs and the engine bed structure based

Konversi Energi dan Manufaktur
P-ISSN : 2339-2029
E-ISSN : 2622-5565
Jurnal Konversi Energi dan Manufaktur
Volume 11 Number 2 – July 2026 Page 170-181
Website : http://journal.unj.ac.id/unj/index.php/jkem
DOI: https://doi.org/10.21009/JKEM.11.2.7

on field data, along with four geometric variations developed from these actual dimensions. The placement of the skegs before and after the modification is illustrated in Figure 5, top and bottom, respectively.

Table 3 presents the specifications for the various skeg sizes, which include the pre-modification actual field data and four other skeg size variations. The determination of these alternative skeg variations was conducted through a comparative analysis referencing the actual post-modification skeg dimensions, which in this study is designated as variation 1. Meanwhile, the detailed dimensions and visual layout of the skeg sizes are shown in Figure 6.

To ensure a systematic investigation, the four skeg variations were developed based on a parametric study of two primary geometric variables: the longitudinal extension length (L_s) and the profile angle of attack (α). The design rationale focused on minimizing pressure drag by streamlining the flow toward the propeller disc while adhering to structural constraints, such as maintaining minimum clearance for the rudder and propeller assembly. Before modification design served as the baseline, while variations 1 through 4 implemented incremental adjustments to the skeg trailing edge profile and volume distribution. This parametric approach allowed for a controlled analysis of how specific geometric changes influence stern flow separation and wake field characteristics. It ensures that the identified optimal design is the result of a structured optimization process rather than arbitrary selection.

Table 3. Skeg dimension (mm)

Description	A	B	C	D	E	F	G
Before modification	300	150	2500	1964	528	3421	4049
Variation 1	450	150	3200	3262	100	8700	8983
Variation 2	425	150	3200	3205	100	8800	8983
Variation 3	515	150	3000	3003	100	8300	8429
Variation 4	350	150	3500	3593	100	9000	9814

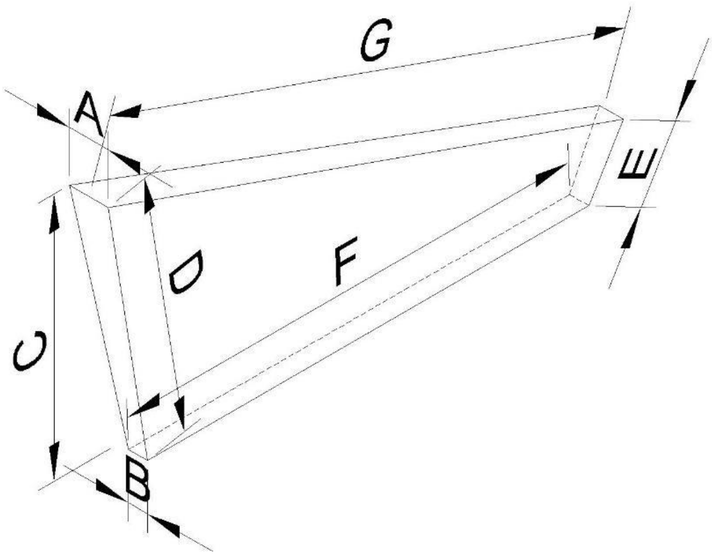

Figure 6. Skeg dimension description

2.5. Model Validation

This stage involves validating the hull model developed using Maxsurf Modeller Advance. Model validation is conducted to ensure that the digitally generated geometry accurately corresponds to or closely matches the actual field conditions. The validation process is performed by comparing the parameters from manual calculations against the values obtained from the software modeling. The maximum allowable error threshold or correction limit for this validation is set to less than 5% across all tested parameters.

The parameters utilized for the hull model validation include displacement volume, block coefficient (C_b), and longitudinal center of buoyancy (LCB). Meanwhile, the parameter used to validate the skeg models is the volume ratio of each skeg variation relative to the actual post-modification skeg volume. It is represented by skeg variation 1.

The first model validation is conducted on the hull modeling results, both for the pre-modification condition and after the modifications, which include changes to the shape and the extension of the stern length. Table 4 presents the error correction results for the hull model validation phase based on the predefined parameters.

Table 4. Skeg modeling validation

Model	Calculation			Modeling			Correction (%)		
	Vol.disp	LCB	C_b	Vol.disp	LCB	C_b	Vol.disp	LCB	C_b
Before	7477.599	46.057	0.85	7487.234	46.569	0.853	0.129	1.112	0.353
After	7758.716	47.519	0.86	7738.583	48.739	0.855	0.259	2.567	0.581

If the values of all parameters do not exceed the established error threshold, the hull model validation process is declared valid, and the study can proceed to the next stage. The subsequent validation phase involves the skeg models. The parameter utilized for the skeg model validation is the skeg volume of each predefined variation, which is compared against the skeg volume of variation 1 (where variation 1 represents the actual skeg dimensions obtained from field data). Table 5 displays the correction results for the skeg model validation stage.

Table 5. Skeg modification modeling validation

Model	Volume (m^3)	Correction (%)
Before modification	3.906	-
Variation 1	6.610	-
Variation 2	6.660	0.751
Variation 3	6.609	0.015
Variation 4	6.617	0.106

3. Results and Discussion

Following the completion of the CFD simulations for all hull models, both pre- modification and post-modification, varying values for drag force and fluid velocity (Velocity U) were obtained for each configuration. The simulations were executed under uniform operational and environmental parameters, specifically at a vessel service speed of 8 knots and an identical water depth. The numerical results from all simulated models are subsequently analyzed and discussed to determine which design variation exhibits hydrodynamic characteristics closest to the pre-modification baseline performance.

To verify the accuracy of the numerical model, the baseline total resistance values obtained from the CFD simulations were validated against empirical predictions calculated using the Holtrop-Mennen method. The comparative analysis, as summarized in Table 6, demonstrates a strong correlation between the numerical simulations and empirical estimations, with a variance of about 4.4% at the service speed of 8 knots. This alignment with established empirical standards confirms that the numerical model successfully captures the hydrodynamic resistance characteristics of the hull.

Konversi Energi dan Manufaktur

Jurnal Konversi Energi dan Manufaktur
Volume 11 Number 2 – July 2026 Page 170-181
Website : http://journal.unj.ac.id/unj/index.php/jkem

P-ISSN : 2339-2029
E-ISSN : 2622-5565
DOI: https://doi.org/10.21009/JKEM.11.2.7

Table 6. Skeg modification validation against empirical estimation

Model	Empirical (kN)	Simulation (kN)	Difference (%)
Before modification	114.476	118.700	3.6%
Variation 1	88.190	83.840	-5.2%
Variation 2	88.253	83.220	-6.0%
Variation 3	88.178	83.090	-6.1%
Variation 4	88.285	81.590	-8.2%

3.1. Drag Force Analysis

The structural modifications performed on the vessel's stern, along with the introduction of various skeg configurations, resulted in distinct drag force values across the different models. Figure 7 outlines the comprehensive drag force data obtained from the CFD simulations for all tested configurations.

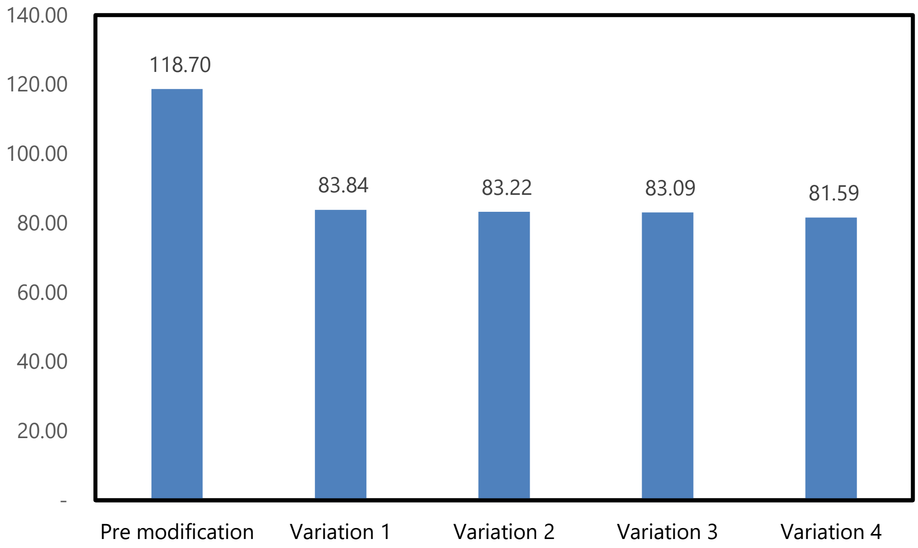

Figure 7. Drag force variations

Based on the graph above, a clear reduction in drag force can be observed between the pre-modification and post-modification states. The pre-modification baseline model exhibits a drag force of 118.70 kN. When compared to the average drag force of the post-modification models, which stands at 82.93 kN, it represents a substantial and significant reduction in resistance. Meanwhile, the differences in values and graphical trends among the various post-modification models themselves are relatively small.

The graph further details the discrepancies in drag force among the modified configurations, where variation 1 presents the highest drag force at 83.84 kN. Conversely, variation 4 yields the lowest drag force at 81.59 kN compared to the other variations. Additionally, a negative sign was observed in the numerical simulation results, indicating that the direction of generated force acts in opposition to the vessel's forward motion. It accurately replicates the hydrodynamic resistance encountered by a ship underway.

3.2. Fluid Velocity Analysis

Similar to the variations in drag force observed before and after modification, as well as across the alternative designs, the fluid velocity (Velocity U) values also exhibit distinct characteristics. Figure 8 presents the Velocity U data obtained from the CFD simulations across three primary regions of the vessel: the bow, the hull (midbody), and the stern.

Konversi Energi dan Manufaktur

P-ISSN : 2339-2029
E-ISSN : 2622-5565

Jurnal Konversi Energi dan Manufaktur
Volume 11 Number 2 – July 2026 Page 170-181
Website : http://journal.unj.ac.id/unj/index.php/jkem
DOI: https://doi.org/10.21009/JKEM.11.2.7

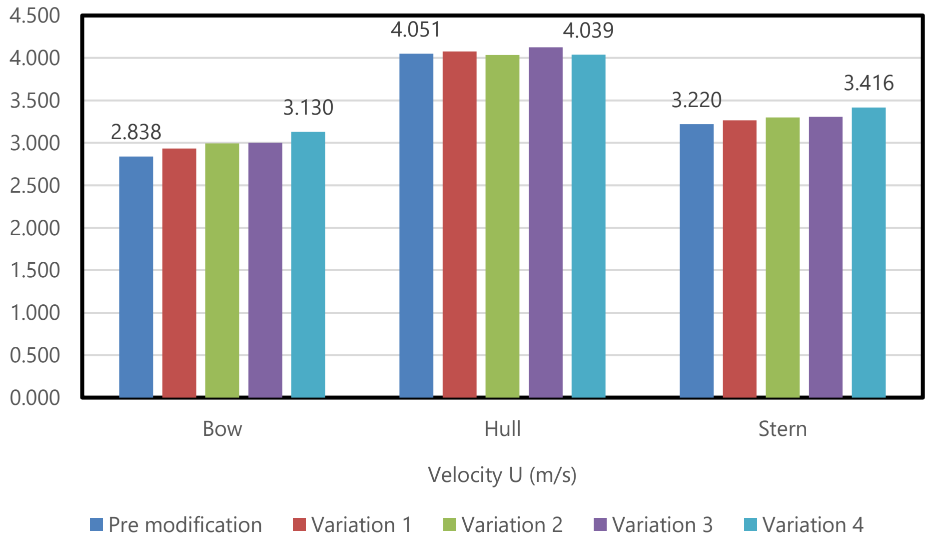

Figure 8. Velocity u variations

Based on the plotted graphs of Velocity U values across the three primary regions, the fluid velocity along the hull increases significantly compared to the bow, before decreasing again as it reaches the stern region. The increase along the hull occurs because the fluid velocity in this region closely approaches the simulated vessel service speed of 8 knots (converted to 4.115 m/s). Conversely, the reduction at the stern is attributed to flow pattern alterations and fluid interaction after passing the main hull body. Nonetheless, the primary focus of this study is directed at the stern region, given that the analysis centers on the effects of stern geometry modifications. Consequently, the Velocity U at the stern serves as the primary parameter for data analysis.

Based on the graphical results of Velocity U at the vessel's stern, distinct differences are observed between the pre-modification and post-modification conditions. The pre-modification baseline Velocity U is 3.220 m/s, whereas the post-modification configurations exhibit varying values across each design. The detailed variation in Velocity U at the stern can be observed in Figure 8, where variation 4 demonstrates the highest Velocity U compared to the other configurations, reaching a value of 3.461 m/s.

3.3. Selection of Optimal Skeg Variation

Following the analysis and comparison of each design configuration, the optimum skeg variation for the modified stern can be determined. The selection process is based on numerical performance indicators, specifically drag force and fluid velocity (Velocity U), referenced against the baseline performance of the pre-modification model. A summary of the primary parameters guiding the selection of the optimum skeg variation is presented in Figure 9.

The optimized geometric profile of variation 4, which considerably lessens flow separation and pressure drag at the stern, is responsible for its higher hydrodynamic performance. The design efficiently delays boundary layer separation at the trailing edge and reduces the strength of turbulent stern vortices that define the baseline model by offering a smoother longitudinal transition. Additionally, improved curvature guarantees a more consistent velocity distribution toward the propeller disc, enhancing wake field properties and lowering energy losses related to eddy formation. These advances in fluid dynamics show that the decrease in overall resistance is not only numerical, but also the outcome of improved flow attachment and more efficient pressure distribution.

Konversi Energi dan Manufaktur

P-ISSN : 2339-2029
E-ISSN : 2622-5565

Jurnal Konversi Energi dan Manufaktur
Volume 11 Number 2 – July 2026 Page 170-181
Website : http://journal.unj.ac.id/unj/index.php/jkem
DOI: https://doi.org/10.21009/JKEM.11.2.7

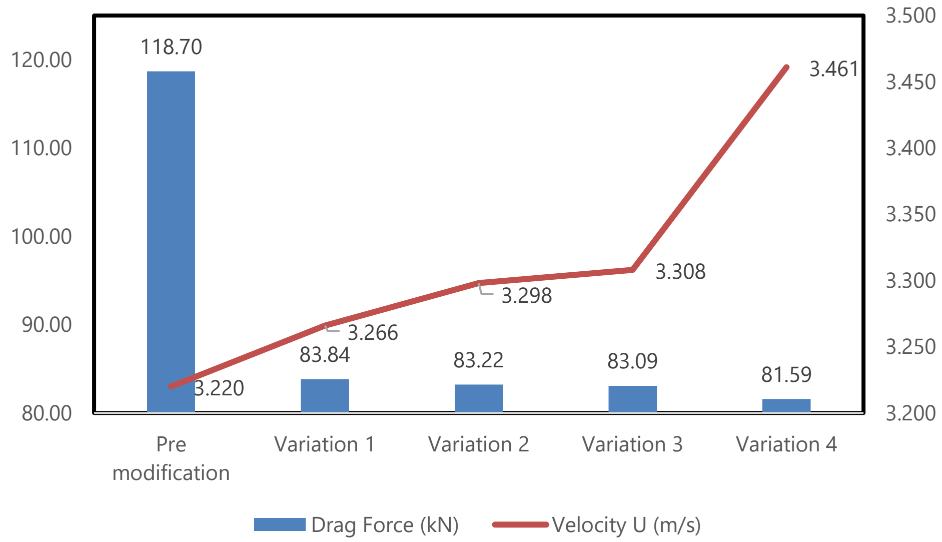

Figure 9. Skeg variations

Based on the graphical data in Figure 9, the optimal variation is determined through a combined evaluation of drag force and fluid velocity. A prior study by Widodo et al. [21] concerning skeg model variations on self-propelled barges concluded that the optimal skeg configuration is characterized by the minimum drag force and the maximum fluid velocity (Velocity U). Adhering to these criteria, variation 4 is identified as the optimal design regarding drag force, as it yields the lowest resistance compared to the other configurations, with a value of 81.59 kN.

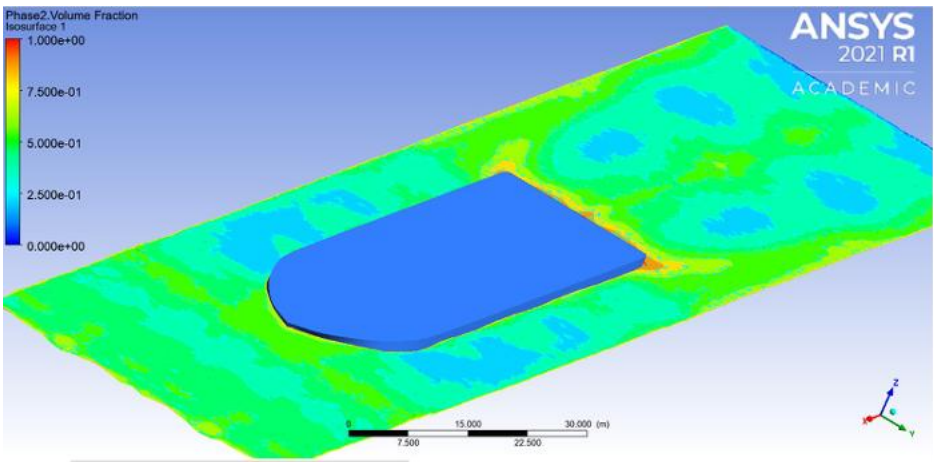

Figure 10. Visual contour in variation 4

Furthermore, evaluating the fluid velocity parameter also position variation 4 as the optimal choice, as it exhibits the highest Velocity U at 3.461 m/s. The visual outputs and flow contours for variation 4, established as the most optimal configuration, are presented in Figure 10 above.

4. Conclusion

This study successfully evaluated the effects of stern geometry modifications and alternative skeg designs on the vessel's hydrodynamic performance utilizing CFD simulations. The numerical results indicate that modifying the stern section significantly reduces the vessel's total resistance (drag force) from a baseline of 118.70 kN to a post-modification average of 82.93 kN. Among the four configurations tested, skeg variation 4 was identified as the optimal design. It yields the minimum drag force of 81.59 kN while simultaneously maximizing the fluid velocity (Velocity U) at the stern region to 3.461 m/s and outperforms variation 1, which exhibited the highest resistance (83.84 kN) and the lowest fluid velocity (3.226 m/s). This finding offers a novel contribution to existing knowledge by demonstrating that integrating an extended stern with an optimized skeg geometry can minimize total resistance by approximately 31.2% compared to the conventional baseline. This decrease in resistance is a critical factor in marine engineering, as lower resistance directly correlates with reduced power requirements to maintain a specific service speed, which potentially improves overall propulsion efficiency and lowers operational fuel consumption.

For future research, it is highly recommended to incorporate the vessel's superstructure into the CFD simulation model to capture total resistance values that more accurately reflect real-world sea states. Additionally, subsequent studies should expand the range of operational vessel speeds and systematically evaluate the influence of the numerical towing tank domain size to construct a more comprehensive hydrodynamic resistance curve. Finally, integrating a ship maneuverability analysis into the post-modification evaluation is essential to ensure that the achieved resistance reduction at the stern does not compromise the vessel's stability and directional handling qualities during service.

5. Acknowledgments

The authors gratefully acknowledge Politeknik Perkapalan Negeri Surabaya, specifically the Ship Design and Construction study programs, for providing the computational facilities and technical support for this research. Special thanks are extended to our industry partners for supplying the essential field data and to colleagues for their invaluable guidance throughout the CFD simulations and manuscript preparation.

6. References

[1] P. Khorsandi and A. Hajivand, "AI-driven ship resistance prediction using three key hydrodynamic parameters," *International Journal of Maritime Technology*, vol. 21, no. 1, pp. 71–79, 2025, doi: 10.61882/ijmt.21.1.71.

[2] A. Buonomano, G. Del Papa, G. F. Giuzio, R. Maka, A. Palombo, and G. Russo, "Design and retrofit towards zero-emission ships: decarbonization solutions for sustainable shipping," *Renewable and Sustainable Energy Reviews*, vol. 213, p. 115384, 2025, doi: 10.1016/j.rser.2025.115384.

[3] B. Ali and L. Ali, "A new concept for design of the shape ship stern," *Global Journal of Information Technology*, vol. 6, no. 1, pp. 18-26, 2016, doi: 10.18844/gjit.v6i1.385.

[4] K. Song, C. Guo, C. Wang, C. Sun, P. Li, and W. Wang, "Numerical analysis of the effects of stern flaps on ship resistance and propulsion performance," *Ocean Engineering*, vol. 193, p. 106621, 2019, doi: 10.1016/j.oceaneng.2019.106621.

[5] Ratson Shipbuilding, "Self-propelled oil barges: an overview of their functionality and benefits," https://www.ratson.com/en/home/infocenterdetail/id/76, 2023 (accessed 10 May 2026).

[6] A. A. Firmansyah, Sutoyo, Arleiny, and T. Pribadi, "Identification and solutions for cargo loss on self-propelled oil barge (SPOB) seroja V," *Journal of Engineering Science and Technology Management*, vol. 6, no. 1, p. 349-358, 2026, doi: 10.31004/jestm.v6i1.407.

[7] F. I. Abdullah, "Kapal tanker ratu yamani terbakar di perairan taboneo, 12 ABK dievakuasi," https://www.beritasatu.com/nusantara/1056939/kapal-tanker-ratu-yamani-terbakar-di-perairan-taboneo-12-abk-dievakuasi, 2023 (accessed 10 May 2026).

[8] R. A. Nabawi, B. Syahri, Y. D. Alfana, and D. Fernandez, "Hydrodynamic optimization of a sweptback stern foil for resistance reduction in flat-hull ships: a CFD-based extension of the hull vane concept," *Teknomekanik*, vol. 9, no. 1, pp. 110–120, 2026, doi: 10.24036/teknomekanik.v9i1.54872.

Konversi Energi dan Manufaktur

P-ISSN : 2339-2029
E-ISSN : 2622-5565

Jurnal Konversi Energi dan Manufaktur
Volume 11 Number 2 – July 2026 Page 170-181
Website : http://journal.unj.ac.id/unj/index.php/jkem DOI: https://doi.org/10.21009/JKEM.11.2.7

[9] A. Firdhaus, Samuel, M. L. Hakim, O. Mursid, and J. R. Putra, “CFD analysis of a stern flap effect on the hydrodynamics of a catamaran ship,” *Scientific Journal of Maritime Research [Pomorstvo]*, vol. 40, no. 2, pp. 165–176, 2026, doi: 10.31217/p.40.2.1.

[10] Romadhoni, B. Santoso, and M. A. Hafiz, “Intelligent optimization of fast boat hull form for resistance reduction using CFD and surrogate-assisted algorithms,” *International Journal of Marine Engineering Innovation and Research*, vol. 11, no. 1, pp. 139–146, 2026, doi: 10.12962/j25481479.v11i1.

[11] M. Iqbal, M. Terziev, T. Tezdogan, and A. Incecik, “Hull form optimisation to minimise the total resistance and dynamic responses of small fishing vessels,” *Ocean Engineering*, vol. 321, p. 120357, 2025, doi: 10.1016/j.oceaneng.2025.120357.

[12] T-. K. Le, N. V. He, N. V. Hien, and N-. T. Bui, “Effects of a bulbous bow shape on added resistance acting on the hull of a ship in regular head wave,” *Journal of Marine Science and Engineering*, vol. 9, no. 6, p. 559, 2021, doi: 10.3390/jmse9060559.

[13] W. Sulistyawati and P. J. Suranto, “Achieving drag reduction with hullform improvement in different optimizing methods,” *International Journal of Technology*, vol. 11, no. 7, pp. 1370-1379, 2020, doi: 10.14716/ijtech.v11i7.4468.

[14] N. K. Im, S. M. Lee, and C. K. Lee, “The influence of skegs on course stability of a barge with a different configuration,” *Ocean Engineering*, vol. 97, pp. 165–174, 2015, doi: 10.1016/j.oceaneng.2015.01.017.

[15] C. Lee and S. Lee, “Effect of skeg on the wave drift force and directional stability of a barge using computational fluid dynamics,” *Journal of Marine Science and Engineering*, vol. 8, no. 11, p. 844, 2020, doi: 10.3390/jmse8110844.

[16] H. Xie, X. Yang, Y. Hu, B. Yang, P. Wei, and W. Liang, “Numerical study on wake wave characteristics around a transom stern vessel,” *Journal of Marine Science and Engineering*, vol. 14, no. 5, p. 482, 2026, doi: 10.3390/jmse14050482.

[17] B-. S. Kim, M-. J. Oh, J-. H. Lee, Y-. H. Kim, and M-. I. Roh, “Study on hull optimization process considering operational efficiency in waves,” *Processes*, vol. 9, no. 5, p. 898, 2021, doi: 10.3390/pr9050898.

[18] H. Jasak, V. Vukčević, I. Gatin, and I. Lalović, “CFD validation and grid sensitivity studies of full scale ship self propulsion,” *International Journal of Naval Architecture and Ocean Engineering*, vol. 11, no. 1, pp. 33–43, 2019, doi: 10.1016/j.ijnaoe.2017.12.004.

[19] S. Adam, G. H. Gebremicheal, R. Swaminathan, S. Mohammed, S. Habtom, S. Huruy, and U. Yassin, “Design and optimization of ship hull for better fuel efficiency,” *International Journal of Science and Research Archive*, vol. 13, no. 1, pp. 029–036, 2024, doi: 10.30574/ijsra.2024.13.1.1526.

[20] M. A. Tariq, Z. M. Mahmood, M. A. Qureshi, N. Khan, M. J. Javaid, and B. Hussain, “CFD-based study of appendages design for dynamic stability of underwater vehicle,” *Journal of Marine Science and Technology*, vol. 30, pp. 658–676, 2025, doi: 10.1007/s00773-025-01075-x.

[21] Widodo, A. Yasim, Rina, and A. Ghofur, “Studi variasi model skeg berdasarkan tahanan dan pola aliran yang melewati lambung barge berpenggerak sendiri,” *Jurnal Wave*, vol. 12, no. 2, pp. 73-80, 2018, doi: 10.29122/jurnalwave.v12i2.3226.